*3rd URSI AT-AP-RASC, Gran Canaria, 29 May – 3 June 2022*

# Indirect Propagation of Body-UAV LoRa Links over Wood and Suburb

Giulio M. Bianco* and Gaetano Marrocco
Pervasive Electromagnetics Lab, University of Rome Tor Vergata, Rome, Italy, http://www.pervasive.ing.uniroma2.it/

## Abstract

The LoRa low-power wide-area protocol has recently been proposed as the enabling technology for a new generation of services and devices for search and rescue (SaR) operations. Consequently, the LoRa terrestrial propagation in a wide range of environments is being characterized worldwide to help design this new family of systems. Still, little is known about body-UAV (unmanned aerial vehicle) channels, especially when the line-of-sight is obstructed. In this contribution, the body-UAV indirect propagation is investigated for the first time through experimental measurements. A log-distance model for links over wood is derived, and the capability of a flying receiver to bypass blockage due to suburban buildings is investigated.

## 1 Introduction

Thanks to the long communication range and low power consumption, the LoRa low-power wide-area protocol recently gained attention for multiple potential applications ranging from healthcare to environmental sensing [1]. LoRa was proven promising for enabling a new generation of devices for search and rescue (SaR) [2] in extremely harsh environments like mountain canyons [3] or woods [4].

Since knowledge on the propagation of signals is essential to optimally deploy networks, a remarkable research effort was devoted to characterizing the LoRa path loss (PL) for different links. The indirect propagation [5] in urban and suburban environments were extensively investigated, e.g. [6, 7], whereas measurements in woods and forest are still relatively scarce. In such environments, the literature is limited to terrestrial LoRa links and reports a reduction of the maximum radio range to a few hundred meters [6, 8, 9] in both the 865 MHz and 433 MHz bands [10]. The vegetation can even negate indirect propagation [11] or create waveguiding effects due to the trees' trunks [12]. Overall, the PL substantially depends on the density, type, and age of the vegetation [13, 14].

Regarding SaR operations, the high mobility of unmanned aerial vehicles (UAV) can significantly speed up operations [15], and knowledge on the propagation of LoRa signals in off-body channels is essential to design effective systems and localization algorithms [16]. The study of this kind of link between wearable devices and UAV is still in its infancy, though [17]. Hence, this contribution reports an experimental characterization of indirect propagation body-UAV of LoRa links in two common non-line-of-sight SaR scenarios: woods and suburbs (Fig. 1). These links have never been investigated before and can be essential to tailor optimized procedures.

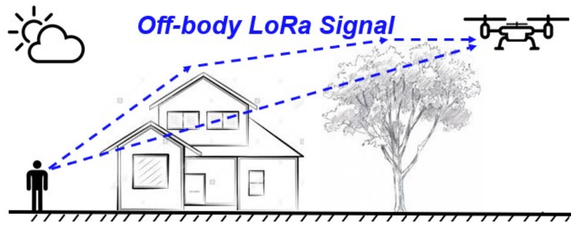


**Figure 1.** Sketch of the body-UAV indirect propagation.

## 2 Modeling Body-UAV Path Loss

Ground-UAV electromagnetic links can be modelled as *i*) angle-dependent w.r.t. an appropriate terrestrial model [18], or *ii*) by a log-distance model depending on the flying height of the UAV [19]. Hereafter, the second approach is employed. Body-UAV channels are off-body ground-UAV links that need special care for modelling the body-worn radio involved by resorting to an equivalent gain evaluated by statistical and numerical analysis [16]. Moreover, the movements of the wearer's body can cause unpredictable polarization losses and body shadowing [3].

For fixed flying height and frequency, the ground-air PL model from [19] reduces to the typical log-distance one,

$$PL(d) = PL(d_0) + n \cdot \log_{10}(d) \tag{1}$$

being $PL(d)$ the mean PL the signal undergoes for a transmitter-receiver distance $d$, $d_0$ a reference distance in the far-field of the transmitter, and $n$ the path loss exponent.

The instantaneous PL $PL_i(d)$ differs from (1) because of small- and large-scale fading. When measuring the $PL_i(d)$ to derive an estimated path loss (EPL) model, multiple measurements in the same point should be performed to average out the small-scale fading $f_{sm}$. Any additional difference between a PL measurement and the EPL is attributed to the

(a) (b)

**Figure 2.** UAV equipped with LoRa receiver. (a) Side view and (b) top view.

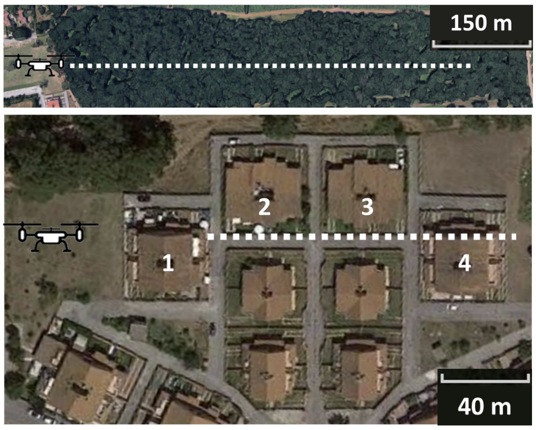


(a)

(b)

**Figure 3.** Satellite view of the flight areas. The position of the UAV and the path walked by the volunteer are reported. (a) Wood and (b) suburb.

zero-mean gaussian shadow fading having standard deviation $\sigma_{SF}$, so that

$$PL_i(d) = PL(d) + f_{sm} + \mathcal{N}\left(0, \sigma_{SF}^2\right) \tag{2}$$

where $\mathcal{N}(\mu, \varsigma)$ denotes a normal distribution with mean $\mu$ and variance $\varsigma$. $PL_i(d)$ can be evaluated by the measured RSSI (received signal strength indicator) and SNR (signal-to-noise ratio) to derive the EPL model through linear fit [3].

Aside from the mean PL of the area, the electromagnetic wave undergoes additional attenuation if it penetrates obstacles. An example is a blockage caused by buildings in urban and suburban areas. The blockage is usually modelled as a jump discontinuity of the mean PL in the point where the obstacle lies, creating a multi-slope model [20], as done in the site-general indoor propagation path loss prediction by the International Telecommunication Union [5]. In the particular case of ground-UAV links, the attenuation caused by the same blockage can depend on the flying height of the UAV.

## 3 Path Loss Measurements

### 3.1 Hardware and Test Area

The LoRa hardware and transmission parameters utilized to perform the following measurements are detailed in [3].

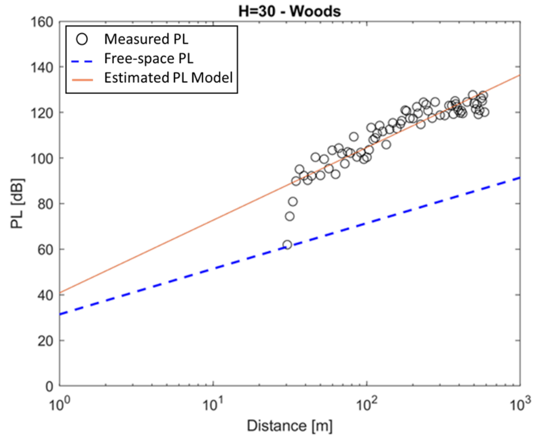


**Figure 4.** Estimated PL model for the body-UAV link over woods when $H = 30$ m.

**Table 1.** Derived path loss model parameters for body-UAV links over the wood.

| **Model (H = 30 m)** | **Woods** | **Free-space** |
|---|---|---|
| **EPL exponent n** | 3.19 | 2 |
| **EPL intercept PL(1 m)** | 40.8 dB | 31.2 dB |
| **Shadow fading $\sigma_{SF}$** | 3.77 dB | - |
| **Number of packets received** | 285 | - |
| **Packet delivery ratio** | 91% | - |

The 868 MHz carrier frequency was used. The employed UAV is a FreeX quadcopter (by Only Flying Machines) where the transmitter was fixed with the dipole forming an approximate angle of 30° with the ground (Fig. 2). A volunteer walked along a planned path with the transmitter inserted in a pocket of their jacket while the UAV was overflying a given point with fixed flying height $H$. The UAV did not change position for the whole duration of the measurements. The receiver in the jacket was properly placed to minimize the polarization losses.

The flight areas selected are a wood and a suburb in Colle Romito (Ardea, Lazio, Italy; GPS coordinates 41°33′01.9”N 12°35′08.4”E; Fig. 3). The wood is mostly composed of poplars (scientific name "populus tremula"). The poplars are adult, not pruned, approximatively tall 10 m, and dense. The suburb is composed of two-storey houses having a side length of about 30 m. As described next, the volunteer firstly hiked in the woods and stationed between the houses as indicated by the white dotted lines in Fig. 3, and then walked all the roads in the suburb. The position of the volunteer was always GPS-tracked. The flights were completed on sunny days of November 2020.

### 3.2 Links over Wood

The volunteer hiked many times from the UAV position and the maximum observed transmitter-receiver communication distance, which is about 590 m. Each measured PL point in Fig. 4 is obtained by averaging five consecutive $PL_i$

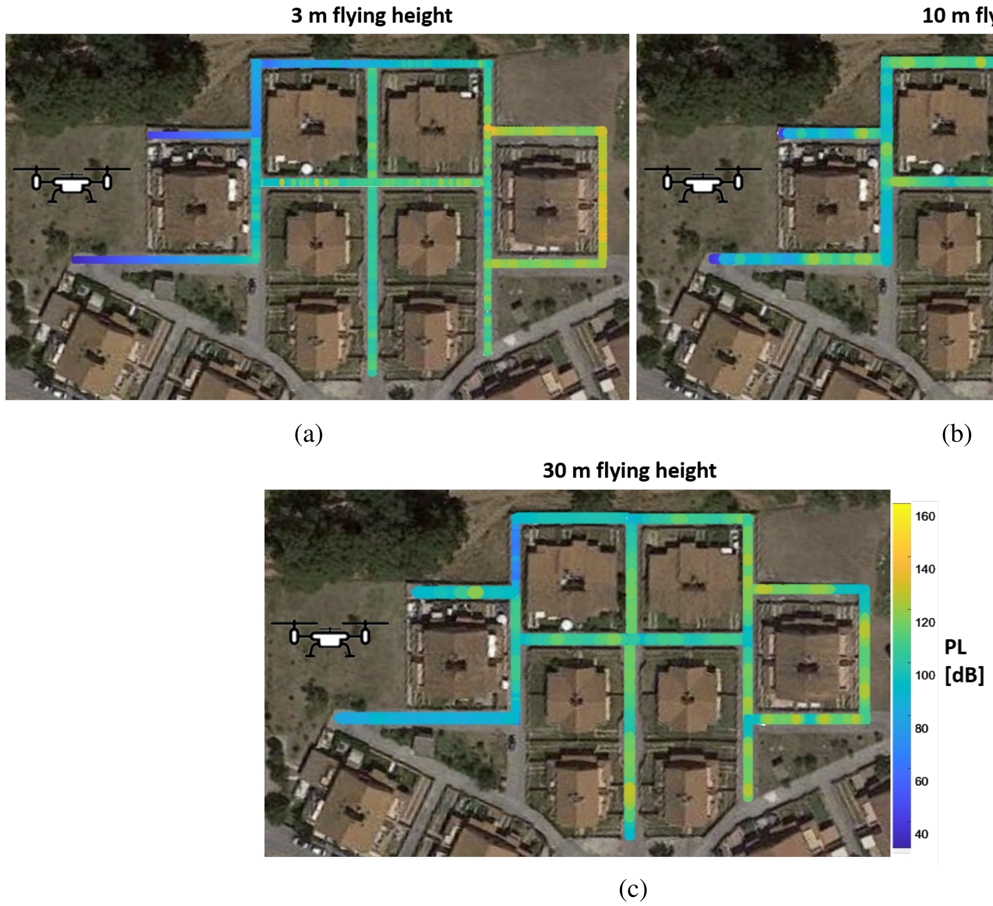


**Figure 5.** Instantaneous PL of the body-UAV LoRa links over a suburb for three flying heights of the UAV: (a) 3 m, (b) 10 m, and (c) 30 m.

collected. For $d > 590$ m, no packet was received until the end of the wood, which extends up to about $d = 720$ m. The log-distance model derived is depicted in Fig. 4, and its parameters are in Table 1.

Overall, a packet delivery ratio of 91% was observed during the data collection in the woods, followed by a sudden drop in the received packets after the maximum radio range. The observation is coherent with the hard degradation of the LoRa signal in areas covered by vegetation reported by the literature. The PL model parameters, instead, are in line with urban and coastal models for LoRa [12].

### 3.3 Links over Suburb

The PL was measured in the suburb for three flying heights, namely 3 m, 10 m, and 30 m. The LoRa transmission was correctly received at every point of the suburb. Fig. 5 shows the propagation of the electromagnetic waves for the three flying heights. The attenuation of the signal measured when the volunteer stayed 3 minutes behind the four buildings is reported in Table 2. From Fig. 5 and Table 2, it is evident that the improved line-of-sight caused by higher $H$ outweighs the longer $d$ only after two buildings, suggesting that the use of the highest transmitters could not be convenient for short-range indirect propagation at LoRa frequencies.

**Table 2.** Attenuation [dB] behind the suburban buildings that are numbered as in Fig. 3(b).

| **Flying height** | $H = 3$ m | $H = 10$ m | $H = 30$ m |
|---|---|---|---|
| **Building 1** | $95 \pm 4.5$ | $110.5 \pm 4$ | $100.6 \pm 3.2$ |
| **Building 2** | $102.2 \pm 2.6$ | $107 \pm 3.8$ | $109.3 \pm 3.3$ |
| **Building 3** | $118.8 \pm 3.7$ | $115.3 \pm 3.5$ | $109.9 \pm 3.5$ |
| **Building 4** | $124.5 \pm 3.9$ | $116.2 \pm 3.7$ | $111.9 \pm 3.4$ |

## 4 Conclusion

In this contribution, the path loss of body-UAV LoRa links over wood and a suburb is experimentally characterized for the first time by means of a UAV-mounted transmitter and a body-worn receiver. The foliage and the buildings mostly negate the line-of-sight yielding to indirect propagation of the waves. A log-distance model for the wood composed of poplars is derived. The vegetation is observed to cause hard degradation of the LoRa signal after just 600 m, a much shorter distance compared with the kilometric communications expected from air-ground direct propagation [16].

Instead, over the suburb area, the transmission is always received, and the flying height can both lower the signal strength by lengthening the ray path or improve the transmission by reducing the building blockage. The findings here exposed can be used to optimize the flying trajectory of UAVs for SaR missions in the woods or suburbs.

## 5 Acknowledgements

The authors thank Ms Giulia Veltro for the support in completing the measurements. The authors also thank professors Franco Mazzenga and Romeo Giuliano for their help throughout the work.

## References

[1] M. Saari, A. Muzaffar bin Baharudin, P. Sillberg, S. Hyrynsalmi, and W. Yan, "LoRa - A survey of recent research trends," *41st Int. Convention Inf. Commun. Technol., Electronics Microelectronics*, 2018, pp. 872–877.

[2] C. Bouras, A. Gkamas, and S. A. K. Salgado, "Energy efficient mechanism for LoRa networks," *Internet Things*, **13**, March 2021, pp. 1-17.

[3] G. M. Bianco, R. Giuliano, F. Mazzenga, and G. Marrocco, A. Mejia-Aguilar, "LoRa system for search and rescue: Path loss models and procedures in mountain scenarios," *IEEE Internet of Things Journal*, **8**, 3, February 2021, pp. 1985–1999.

[4] A. Calabrò and R. Giuliano, "Integrated Wi-Fi and LoRa network on UAVs for localizing people during SAR operations," *Int. Conf. Electrical Electronic Technol. Automotive*, November 2021, pp. 1–6.

[5] J. S. Seybold, *Introduction to RF Propagation*, Hoboken, NJ, USA John Wiley & Sons, 2005.

[6] A. E. Ferreira *et al.*, "A study of the LoRa signal propagation in forest, urban, and suburban environments," *Ann. Telecommun.*, **75**, 2020, pp. 333–351.

[7] T. Ameloot, P. Van Torre, and H. Rogier, "Periodic LoRa Signal Fluctuations in Urban and Suburban Environments," *13th Eur. Conf. Antennas Propag.*, April 2019, pp. 1–5.

[8] M. R. Villarim, J. V. H. de Luna, D. de Farias Medeiros, R. I. S. Pereira and C. P. de Souza, "LoRa performance assessment in dense urban and forest areas for environmental monitoring," *4th Int. Sym. Instrum. Sys., Circuits Transducers*, 2019, pp. 1–5.

[9] G. Callebaut, G. Leenders, C. Buyle, S. Crul, and L. Van Der Perre, "LoRa physical layer evaluation for point-to-point links and coverage measurements in diverse environments," *Eur. Conf. Netw. Commun.*, November 2019, pp. 1-2.

[10] K. A. Ahmad, M. S. Salleh, J. D. Segaran, and F. R. Hashim "Impact of foliage on LoRa 433 MHz propagation in tropical environment," *AIP Conf. Proc.*, February 2018, pp. 1–6.

[11] M. R. Villarim *et al.*, "An evaluation of LoRa communication range in urban and forest areas: A case study in Brazil and Portugal," *IEEE 10th Annual Inf. Technol., Electronics Mobile Commun. Conf*, Vancouver, Canada, 2019.

[12] G. Callebaut and L. Van der Perre, ""Characterization of LoRa point-to-point path loss: Measurement campaigns and modeling considering censored data," *IEEE Internet Things J.*, **7**, 3, March 2020, pp. 1910–1918.

[13] Y. Wu, G. Guo, G. Tian, and W. Liu, "A model with leaf area index and trunk diameter for LoRaWAN radio propagation in eastern china mixed forest," *J. Sensors*, **2020**, June 2020, pp. 1–16.

[14] M. R. Ansah, R. A. Sowah, J. Melà-Segul, F. A. Katsriku, X. Vilajosana, and W. O. Banahene, "Characterising foliage influence on LoRaWAN pathloss in a tropical vegetative environment," *IET Wirel. Sens. Sys.*, **10**, 5, June 2020, pp. 198–207.

[15] D. Erdos, A. Erdos, and S. E. Watkins, "An experimental UAV system for search and rescue challenge," *IEEE Aerospace Electronic Sys. Mag.*, **28**, 5, May 2013, pp. 32–37.

[16] G. M. Bianco, A. Mejia-Aguilar, and G. Marrocco, "Numerical and experimental evaluation of Radiohelmet-to-UAV LoRa links," *XXIVth General Assembly and Scientific Symposium of the International Union of Radio Science*, September 2021, pp. 1–4.

[17] A. Kachroo *et al.*, "Unmanned aerial vehicle-to-wearables (UAV2W) indoor radio propagation channel measurements and modeling," *IEEE Access*, **7**, May 2019, pp. 73741–73750.

[18] A. Al-Hourani and K. Gomez, "Modeling cellular-to-UAV path-loss for suburban environments," *IEEE Wireless Commun. Lett.*, **7**, 1, February 2018, pp. 82–85.

[19] Z. Cui, C. Briso-Rodríguez, K. Guan, C. Calvo-Ramírez, B. Ai, and Z. Zhong, "Measurement-based modeling and analysis of UAV air-ground channels at 1 and 4 GHz," *IEEE Antennas Wireless Propagation Lett.*, **18**, 9, September 2019, pp. 1804-1808.

[20] G. M. Bianco, R. Giuliano, F. Mazzenga, and G. Marrocco, "Multi-slope path loss and position estimation with grid search and experimental results," *IEEE Transactions on Signal and Information Processing over Networks*, **7**, August 2021, pp. 551–561.